Journal of Molecular Modeling (2023) 29:215
https://doi.org/10.1007/s00894-023-05606-4

ORIGINAL PAPER

On the mechanical, electronic, and optical properties of the boron nitride analog for the recently synthesized biphenylene network: a DFT study

F. F. Monteiro[1] · W. F. Giozza[2] · R. T. de Sousa Júnior[2] · P. H. de Oliveira Neto[1] · L. A. Ribeiro Júnior[1] · M. L. Pereira Júnior[2]

Received: 23 February 2023 / Accepted: 26 May 2023 / Published online: 22 June 2023

Abstract

Context Recently, a new 2D carbon allotrope named biphenylene network (BPN) was experimentally realized. Here, we use density functional theory (DFT) calculations to study its boron nitride analogue sheet's structural, electronic, and optical properties (BN-BPN). Results suggest that BN-BPN has good structural and dynamic stabilities. It also has a direct bandgap of 4.5 eV and significant optical activity in the ultraviolet range. BN-BPN Young's modulus varies between 234.4−273.2 GPa depending on the strain direction.

Methods Density functional theory (DFT) simulations for the electronic and optical properties of BN-BPN were performed using the CASTEP package within the Biovia Materials Studio software. The exchange and correlation functions are treated within the generalized gradient approximation (GGA) as parameterized by Perdew-Burke-Ernzerhof (PBE) and the hybrid functional Heyd-Scuseria-Ernzerhof (HSE06). For convenience, the mechanical properties were carried out using the DFT approach implemented in the SIESTA code, also within the scope of the GGA/PBE method. We used the double-zeta plus polarization (DZP) for the basis set in these cases. Moreover, the norm-conserving Troullier-Martins pseudopotential was employed to describe the core electrons.

Keywords Boron Nitride Network · Biphenylene Network · Optoelectronic properties · Mechanical properties · DFT

Introduction

Since the synthesis of graphene in 2004 by Novoselov and coworkers [1], 2D materials have been extensively investigated for developing novel applications in flat electronics [2–4]. Its unique structural, thermal, optical, and electrical properties opened exciting possibilities for breakthroughs in nanotechnology [5–8]. Based on that, several theoretical and experimental studies were performed to propose new 2D materials with similar properties to graphene, which can overcome its zero-gap problem regarding some optoelectronic applications [9–14]. By introducing a band gap, these new 2D materials can be tailored to exhibit desirable optoelectronic properties [15]. No electron states are available in the band gap, which determines the material's ability to control the charge transport and interact with light. A band gap is essential in optoelectronic devices like solar cells [16], photodetectors [17], and light-emitting diodes [18]. Graphene's zero-gap nature limits its ability to efficiently absorb and emit light within specific energy ranges, making it less suitable for these applications.

Researchers usually combine theoretical predictions and experimental validation to identify new 2D materials with suitable band gaps for these purposes [19, 20]. Several promising materials have emerged from these efforts, such as transition metal dichalcogenides [21], black phosphorus (phosphorene) [22], boron nitride monolayers [23], and various hybrid organic—inorganic perovskite structures [24]. These materials possess various electronic properties, tunable bandgaps, and excellent optoelectronic characteristics,

This paper belongs to the Topical Collection IX Symposium on Electronic Structure and Molecular Dynamics - IX SeedMol.

✉ M. L. Pereira Júnior
marcelo.lopes@unb.br

[1] Institute of Physics, University of Brasília, Brasília, Brazil

[2] Faculty of Technology, Department of Electrical Engineering, University of Brasília, Brasília, Brazil

making them potential alternatives to graphene in specific applications.

Materials modelling and design using computational quantum and classical approaches are now essential in materials research [25–28]. Usually, theoretical predictions of new nanostructured materials preceded their synthesis by decades. Such preliminary theoretical studies can open channels for the future synthesis of a particular material. Some examples are the biphenylene network [29, 30] and 2D polymerized fullerenes [31, 32].

In recent *in-silico* studies, several boron nitride 2D materials have been proposed. These materials have a similar topology to some carbon-based monolayers that have already been synthesized. Examples include graphene (h-BN) [33–35], monolayer amorphous carbon (binary monolayer amorphous boron nitride) [36, 37], penta-graphene (penta-BN) [38, 39], T-graphene (T-BN) [33, 40], and phagraphene (pha-BN) [41, 42]. Additionally, the boron nitride form of the biphenylene network (BPN) [30], called BN-BPN, was proposed through in-silico studies by Mortazavi [43] and co-workers and also in other computational studies [43–46], but it is still needed to explore its structural and mechanical properties. Our study also extends the investigation of BN-BPN to include electronic and optical properties, utilizing a hybrid DFT functional.

The naming of carbon allotropes, particularly in two-dimensional (2D) carbon materials, has posed challenges due to their growing diversity and complexity. Reference [47] emphasizes the importance of a clear description for this group of materials, which encompasses more than monolayer graphene. Furthermore, the reference [47] recommends employing descriptive and scientifically precise terminology to characterize material structures. Due to this reason, we have chosen to retain the original name of the carbon structure under investigation in this study (the biphenylene network) while referring to a boron nitride variant with a comparable topology.

In this work, we use DFT calculations to computationally study the mechanical, electronic, and optical properties of the BN-BPN. Our *in-silico* strategy revealed the absence of negative frequencies in the phonon spectrum, confirming its structural stability. Moreover, we found that BN-BPN has a direct bandgap of 4.5 eV and significant optical absorption in the ultraviolet range. BN-BPN Young's Modulus varies between 234.4−273.2 GPa depending on the strain direction.

Methodology

The DFT simulations for the electronic and optical properties of BN-BPN (see Fig. 1) were performed using the CASTEP package [48] within the Biovia Materials Studio software [49]. The exchange and correlation functions are

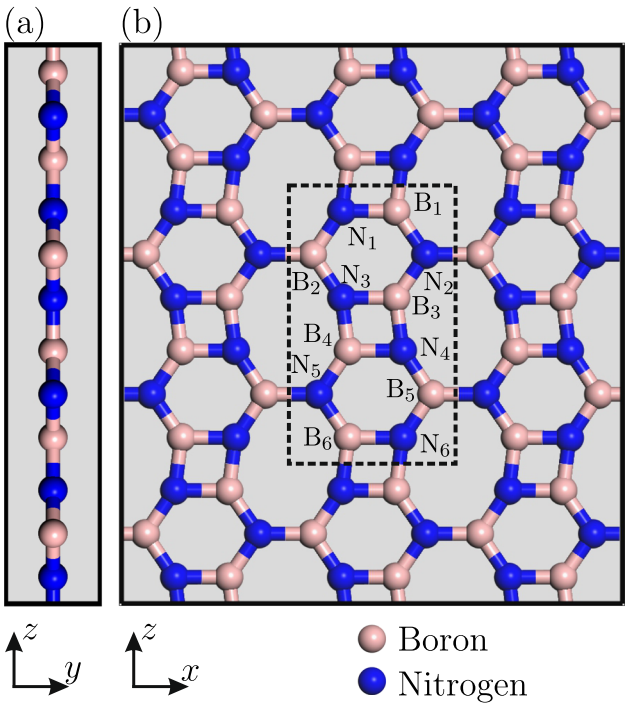

Fig. 1 Schematic representation of **a** side and **b** front views of the BN-BPN monolayer. The dashed lines highlight the lattice unit cell. The labelled atoms with the unity cell stand different bonds

treated within the generalized gradient approximation (GGA) as parameterized by Perdew-Burke-Ernzerhof (PBE) [50] and the hybrid functional Heyd-Scuseria-Ernzerhof (HSE06) [51]. We used the norm-conserving pseudopotentials for boron and nitrogen provided in Biovia Materials Studio.

We used 500 eV as the energy cutoff of the plane wave basis set and convergence criteria of 1.0×10^{-5} eV for energy. BN-BPN lattice was fully relaxed until the residual force on each atom was less than 1.0×10^{-3} eV/Å, using periodic boundary conditions. The basis vector along the z-direction was fixed during the lattice optimization. The k-grid is $10 \times 10 \times 1$ for geometry optimization and $20 \times 20 \times 1$ for electronic and optical calculations. A vacuum region of 20 Å was considered to prevent spurious interactions among the BN-BPN layers. The phonon calculations used the linear response method [52] with a grid-spacing of 0.05 1/Å and a convergence tolerance of 10^{-5} eV/Å^2.

For convenience, the mechanical properties were investigated using the DFT approach implemented in the SIESTA code [53] within the scope of the GGA/PBE [50] method. We used the double-zeta plus polarization (DZP) for the basis set. Norm-conserving pseudopotentials were employed to describe the core electrons, as available in Pseudo DOJO [54]. We used a kinetic energy cutoff of 500 eV and a $6 \times 6 \times 1$ k-grid.

GGA functionals provide a better electronic subsystem description than LDA functionals. LDA tends to overbind

atoms, resulting in underestimated bond lengths and cell volume and overestimated bulk modulus. GGA corrects this error but may underbind, causing slightly longer bond lengths. PBE is an exchange-correlation (XC) functional that underestimates band gaps. In contrast, HSE06 is a hybrid XC functional that considers long-range electron—electron interactions and is highly accurate in predicting band gap values.

The optical coefficients derive from the complex dielectric function. An external electric field of value 1.0 V/Å (oriented in the normal direction to the material surface) was applied to estimate the coefficients. A detailed description of the procedure to calculate the optical properties (used in this work) is given in the reference [55].

Results

We first describe the lattice arrangement for the optimized BN-BPN sheet, as shown in Fig. 1. Calculations for HSE06 level yield B-N bond distances and N-B-N angles varying between 1.44−1.48 Å and 83.06−153.18°, respectively (see Table 1). As expected, the BN-BPN lattice has similar optimized parameters when calculated using GGA/PBE and HSE06 methods. For this reason, we present Fig. 3 and Table 1, just the optimized parameters obtained using HSE06.

Figure 1 illustrates that the four- and eight-membered rings are distorted when contrasted with all-carbon BPN [32, 56, 57], but the lattice is still planar. The BN-BPN lattice is orthorhombic and belongs to the space group PMMA (D2H-5). This negative value for the cohesive energy suggests that the free-standing state of BN-BPN is likely to be stable.

Table 1 BN-BPN bond distances and angles for calculations using the HSE06 level. The atom labels are highlighted in Fig. 1

Atoms		Distance [Å]
$N_1B_2/N_3B_2/N_4B_5/N_6B_5$		1.44
$N_2B_1/N_2B_3/N_5B_4/N_5B_6$		1.44
$N_1B_6/B_1N_6/N_3B_4/B_3N_4$		1.46
N_2B_2/N_5B_5		1.47
$N_1B_1/N_3B_3/N_4B_4/N_6B_6$		1.48
Atoms	Angle °	Ring
$N_3B_3N_4/B_4N_3B_3$	83.06	4-atoms
$B_3N_4B_4/N_4B_4N_3$	96.94	4-atoms
$B_1N_2B_3$	110.52	6-atoms
$N_3B_2N_1$	112.00	6-atoms
$B_3N_3B_2/B_2N_1B_1$	123.76	6-atoms
$N_2B_2N_3/N_5B_5N_4$	124.00	8-atoms
$B_3N_2B_2/B_4N_5B_5$	124.74	8-atoms
$N_1B_1N_2/N_2B_3N_3$	124.98	6-atoms
$B_2B_4N_5/N_4B_3N_2$	138.08	8-atoms
$B_2N_3B_4/B_5N_4B_3$	153.18	8-atoms

The dynamical stability of the BN-BPN sheet was examined by calculating the phonon dispersion relations along the high symmetry directions, as depicted in Fig. 2(a). The PDPS diagram (see Fig. 2(b)) reveals the absence of a band gap between acoustic and optical modes, indicating a high scattering process rate and a short phonon lifetime. This result suggests that BN-BPN has a relatively low lattice thermal conductivity. On the other hand, the presence of only real frequencies in the phonon dispersion profile indicates its good dynamical stability.

Figure 3 presents the electronic band structure and corresponding projected density of states (PDOS) for the BN-BPN sheet using the GGA/PBE (Fig. 3(a) and (b)) HSE06 approaches. In Fig. 3(a) and (b), one can note that BN-BPN has a direct bandgap, at Γ-point, of 3.17 eV and 4.53 eV, on the GGA/PBE and HSE06 levels, respectively. In these cases, the DOS is predominantly formed by $2p$ atomic orbitals. BN-BPN is an insulating material even at GGA/PBE level. Generally, calculations at the GGA-PBE level tend to underestimate bandgaps compared to the ones at the HSEO6 level. The electronic structure of BN-BPN and other 2D-BN allotropes were studied in the nanoribbons, sheets, and bulks forms [43, 46]. As a general trend, their band structure presented a band gap of 3.2 eV on the GGA/PBE. This result agrees with the band gap value in Fig. 3(a).

Now, we turn to the optical properties of BN-BPN. Figure 4(a) presents the refractive index (n) and extinction coefficient (k), as a function of the photon energy, for an unpolarised light beam (oriented in the normal direction to the material surface) and a scissor operator of 1.36 eV. The inset panel, Fig. 4(b), shows the BN-BPN optical absorption as a function of the photon energy. In these figures, one can note that the intense optical activity of BN-BPN is

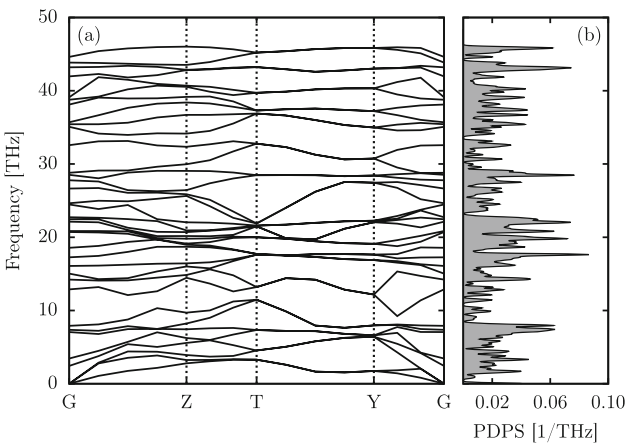

Fig. 2 Phonon band structure of BN-BPN at GGA/PBE level

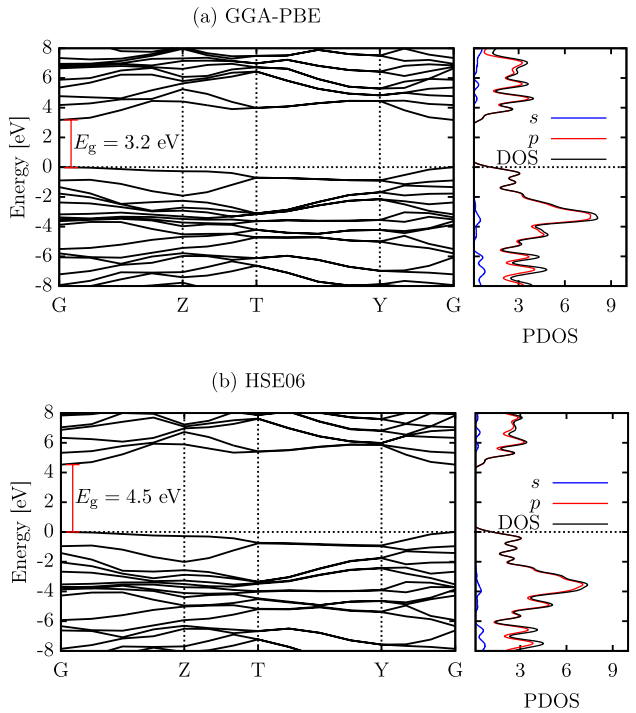

Fig. 3 Electronic band structure and corresponding projected/total density of states (PDOS/DOS) for BN-BPN sheet. These results were obtained using the **a** GGA/PBE and **b** HSE06 approaches

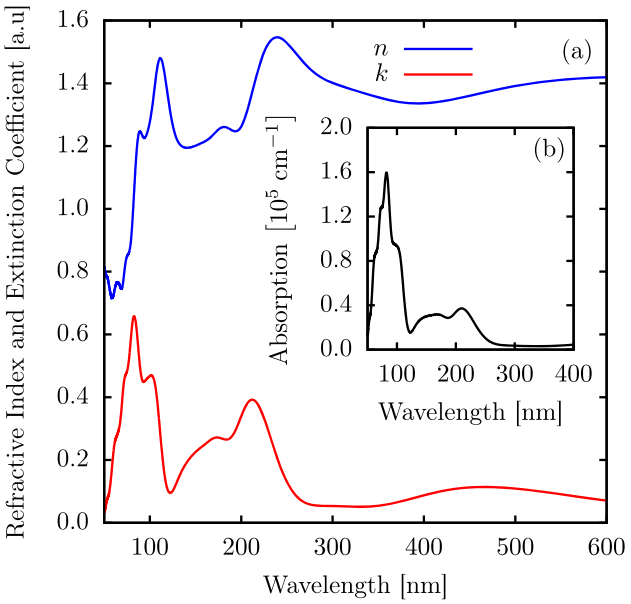

Fig. 4 **a** Refractive index (n) and extinction coefficient (k) and **b** absorption coefficient as a function to the photon energy, at GGA/PBE level, for an unpolarised light beam (oriented in the normal direction to the material surface)

restricted to the ultra-violet region. The refractive index has two well-defined peaks at 112 nm and 239 nm. The absorption coefficient in Fig. 4(b) has one pronounced peak at 82 nm and a shallow peak at 214 nm. This optical activity trend suggests that BN-BPN will appear colourless (or transparent) in solution. Moreover, it can be a good candidate for UV device collectors. Notably, the extinction coefficient also has two well-defined peaks at 82 nm and 214 nm, following the trend presented by the absorption coefficient by determining how strongly BN-BPN absorbs radiation.

Finally, we discuss the mechanical properties of BN-BPN. We used a cell of 7.68×9.12 Å^2, formed by replicating the unit cell in Fig. 1 by $2 \times 2 \times 1$. Figure 5 presents the stress–strain curve under uniaxial strain loading along the x and y directions (blue and red circles, respectively). Here, we show the stress–strain interplay until the moment of the lattice fracture. As a general trend, the BN-BPN lattice has two well-defined stages for the stress–strain relationship, i.e., elastic and fractured. The BN-BPN Young's modulus values along the x- and y-directions are calculated in the linear regime up to 5% of strain.

In the elastic regime, the stress rises almost linearly up to 10% of strain in both directions. The BN-BPN lattice remains cohesive in this regime, but its rings deformed during stretching. Between 10–18% and 10–16% of strain in the x- and y-direction, respectively, the BN-BPN lattice suffers its first bond breaking, producing a crack. Above these critical strain thresholds (fractured stage), the crack propagates rapidly, and the stress drops abruptly to zero, indicating the rupture of the BN-BPN lattice. The estimated elastic moduli are 273.2 GPa and 234.4 GPa for the applied strain in the x- and y-direction, respectively. These values are substantially smaller than what was reported by the all-carbon BPN (about 1019.4 GPa) [58]. The fracture strain (σ_C) and ultimate stress (ϵ_C) are $\sigma_C = 18$ % and $\epsilon_C = 83.7$ GPa in the x-direction and $\sigma_C = 16$ % and $\epsilon_C = 69.8$ GPa in the y-direction. σ_C is obtained from the strain percentage corresponding to the higher stress value,

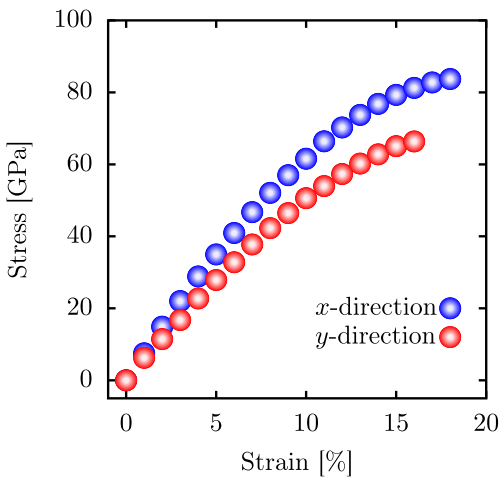

Fig. 5 Stress–strain relationships of BN-BPN under uniaxial tensile loading in (blue) the x-direction and (red) y-direction

i.e., ϵ_C. One can note that BN-BPN has anisotropic mechanical properties, as expected from its lattice arrangement.

In terms of mechanical response, BPB-BN behaves as a common elastic material. A uniaxial compressive strain (negative strain) is applied in one of its plane directions, and the BPN-BN contracts (elongates) in the direction of the applied strain while simultaneously elongating (contracting) in the perpendicular direction. The BPN-BN is not auxetic, as can be inferred from MD and DFT simulations for the all-carbon BPN [58, 59], and has a positive Poisson's ratio of about 0.254. The Poisson's ratio of graphene and hBN are 0.165 and 0.211 [60], respectively.

Conclusions

In summary, we conducted DFT simulations to study the electronic, optical, and dynamical properties of the boron nitride analogue sheet (BN-BPN) for the all-carbon BPN. To examine its structural stability, we calculated the phonon spectrum. All calculated phonon frequencies are positive, thus confirming the BN-BPN stability. The highest phonon frequency is about 47 THz, similar to graphene and all carbon BPN, indicating the predominance of p-hybridized boron-nitride bonds.

Concerning the electronic structure, we obtained that BN-BPN has a direct bandgap, at Γ-point, of 3.17 eV and 4.53 eV, on the GGA/PBE and HSE06 levels, respectively. In these cases, the DOS is predominantly formed by $2p$ atomic orbitals. BN-BPN is an insulating material even at the GGA/PBE calculation level. The intense optical activity of BN-BPN is restricted to the ultra-violet region.

BN-BPN has in-plane anisotropic mechanical properties, as expected from its topology. The estimated elastic moduli are 273.2 GPa and 234.4 GPa for the applied strain in the x- and y-direction, respectively. These values are substantially smaller than what was reported by the all-carbon BPN (about 1019.4 GPa). The BPN-BN is not auxetic and has a positive Poisson's ratio of about 0.254.

Acknowledgements The authors gratefully acknowledge the financial support from the Brazilian Research Councils CNPq, CAPES, and FAPDF. L.A.R.J acknowledges the financial support from Brazilian Research Council FAP-DF grants 00193 − 00001247/2021 − 20, 00193 − 00000857/2021 − 14, CNPq grants 302236/2018 − 0 and 350176/2022 − 1, and FAP-DF-PRONEM grant 00193.00001247/2021 − 20. F.F.M and W.F.G acknowledge the financial support from FAP-DF grants 00193.00001808/2022 − 71 and 00193 − 00000811/2021 − 97, respectively. This study was financed in part by the Coordenação de Aperfeiçoamento de Pessoal de Nível Superior - Brasil (CAPES) - Finance Code 88887.691997/2022-00. M.L.P.J and L.A.R.J. acknowledge CENAPAD-SP for providing computational facilities. R.T.S.J. gratefully acknowledges CNPq (Grants 312180/2019-5 PQ-2 and 465741/2014-2 INCT on Cybersecurity). R.T.S.J. and L.A.R.J. gratefully acknowledge the support from ABIN grant 08/2019.

R.T.S.J. and L.A.R.J. gratefully acknowledge the support from ABIN grant 08/2019.

Author Contributions F. F. Monteiro: data curation, formal analysis, methodology, and writing—original draft preparation. W. F. Giozza: data curation, formal analysis, methodology, and funding acquisition. R. T. de Sousa Júnior: formal analysis, methodology, and funding acquisition. P. H. de Oliveira Neto: data curation, formal analysis, and methodology. L. A. Ribeiro Júnior: conceptualization, funding acquisition, and writing—reviewing and editing. M. L. Pereira Júnior: data curation, supervision, formal analysis, methodology, prepared figures, and writing—reviewing and editing. All authors reviewed the manuscript.

Funding L.A.R.J acknowledges the financial support from Brazilian Research Council FAP-DF grants 00193 − 00001247/2021 − 20, 00193 − 00000857/2021 − 14, CNPq grants 302236/2018 − 0 and 350176/2022 − 1, and FAP-DF-PRONEM grant 00193.00001247/2021 − 20. F.F.M and W.F.G acknowledge the financial support from FAP-DF grants 00193.00001808/2022 − 71 and 00193 − 00000811/2021 − 97, respectively. This study was financed in part by the Coordenação de Aperfeiçoamento de Pessoal de Nível Superior - Brasil (CAPES) - Finance Code 88887.691997/2022-00. M.L.P.J and L.A.R.J. acknowledge CENAPAD-SP for providing computational facilities. R.T.S.J. gratefully acknowledges CNPq (Grants 312180/2019-5 PQ-2 and 465741/2014-2 INCT on Cybersecurity). R.T.S.J. and L.A.R.J. gratefully acknowledge the support from ABIN grant 08/2019. R.T.S.J. and L.A.R.J. gratefully acknowledge the support from ABIN grant 08/2019. R.T.D.S. is supported by CNPq - Brazilian National Research Council (Grant 310941/2022-9 PQ-1D), FAPDF - Brazilian Federal District Research Support Foundation (Grant 625/2022 SISTER City), and the University of Brasilia (Grant 7129 UnB COPEI).

Availability of data and material N/A.

Code Availability N/A.

Declarations

Conflict of interest The authors declare no competing interests.

References

1. Novoselov KS, Geim AK, Morozov SV, Jiang DE, Zhang Y, Dubonos SV, Grigorieva IV, Firsov AA (2004) Science 306(5696):666
2. Wang Z, Dong F, Shen B, Zhang R, Zheng Y, Chen L, Wang S, Wang C, Ho K, Fan YJ et al (2016) Carbon 101:77
3. Allen MJ, Tung VC, Kaner RB (2010) Chem Rev 110(1):132
4. Cassiano TDSA, Monteiro FF, de Sousa LE, e Silva GM, de Oliveira Neto PH (2020) RSC Adv 10(45):26937
5. Renteria JD, Nika DL, Balandin AA (2014) Appl Sci 4(4):525
6. Asha AB, Narain R (2020) In: Polymer science and nanotechnology. Elsevier, pp 343–359
7. Lue JT (2007) Encyclopedia of nanoscience and nanotechnology 10(1):1
8. Saleh TA (2020) Environ Technol Innov 20:101067
9. Kumar R, Singh RK, Singh DP (2016) Renew Sustain Energy Rev 58:976
10. Lima KAL, Cunha WFD, Monteiro FF, Enders BG et al (2019) J Mol Model 25(12):1

11. Nasir S, Hussein MZ, Zainal Z, Yusof NA (2018) Materials 11(2):295
12. Zhu CY, Ye YW, Guo X, Cheng F (2022) New Carbon Mater 37(1):59
13. Monteiro FF, Azevedo DL, da Silva EC, Ribeiro LA Jr, de Almeida Fonseca AL (2015) Chem Phys Lett 636:62
14. Ng YH, Ikeda S, Matsumura M, Amal R (2012) Energy Environ Sci 5(11):9307
15. Peng Z, Chen X, Fan Y, Srolovitz DJ, Lei D (2020) Light Sci Appl 9(1):190
16. Murad AR, Iraqi A, Aziz SB, Abdullah SN, Brza MA (2020) Polymers 12(11):2627
17. Liu F, Shimotani H, Shang H, Kanagasekaran T, Zólyomi V, Drummond N, Fal'ko VI, Tanigaki K (2014) ACS Nano 8(1):752
18. Park NM, Kim TS, Park SJ (2001) Appl Phys Lett 78(17):2575
19. Liu Y, Zhao T, Ju W, Shi S (2017) J Materiomics 3(3):159
20. Alberi K, Nardelli MB, Zakutayev A, Mitas L, Curtarolo S, Jain A, Fornari M, Marzari N, Takeuchi I, Green ML et al (2018) J Phys D Appl Phys 52(1):013001
21. Manzeli S, Ovchinnikov D, Pasquier D, Yazyev OV, Kis A (2017) Nat Rev Mater 2(8):1
22. Morita A (1986) Appl Phys A 39:227
23. Tran TT, Bray K, Ford MJ, Toth M, Aharonovich I (2016) Nat Nanotechnol 11(1):37
24. Li W, Wang Z, Deschler F, Gao S, Friend RH, Cheetham AK (2017) Nat Rev Mater 2(3):1
25. Louie SG, Chan YH, da Jornada FH, Li Z, Qiu DY (2021) Nat Mater 20(6):728
26. Bauer B, Wecker D, Millis AJ, Hastings MB, Troyer M (2016) Phys Rev X 6(3):031045
27. Panchal JH, Kalidindi SR, McDowell DL (2013) Comput Aided Des 45(1):4
28. Butler KT, Frost JM, Skelton JM, Svane KL, Walsh A (2016) Chem Soc Rev 45(22):6138
29. Hudspeth MA, Whitman BW, Barone V, Peralta JE (2010) ACS Nano 4(8):4565
30. Fan Q, Yan L, Tripp MW, Krejčí O, Dimosthenous S, Kachel SR, Chen M, Foster AS, Koert U, Liljeroth P et al (2021) Science 372(6544):852
31. Berber S, Osawa E, Tománek D (2004) Phys Rev B 70(8):085417
32. Hou L, Cui X, Guan B, Wang S, Li R, Liu Y, Zhu D, Zheng J (2022) Nature 606(7914):507
33. Liu L, Feng Y, Shen Z (2003) Phys Rev B 68(10):104102
34. Pacile D, Meyer J, Girit Ç, Zettl A (2008) Appl Phys Lett 92(13):133107
35. Jin C, Lin F, Suenaga K, Iijima S (2009) Phys Rev Lett 102(19):195505
36. Felix LC, Tromer RM, Autreto PA, Ribeiro Junior LA, Galvao DS (2020) J Phys Chem C 124(27):14855
37. Zhang YT, Wang YP, Zhang X, Zhang YY, Du S, Pantelides ST (2022) Nano Lett 22(19):8018
38. Zhang S, Zhou J, Wang Q, Chen X, Kawazoe Y, Jena P (2015) Proc Natl Acad Sci 112(8):2372
39. Li J, Fan X, Wei Y, Chen G (2016) Sci Rep 6(1):1
40. Siqi J, Shasha Y, Xiao W, Gu W (2020) Mol Phys 118(18):e1757775
41. Wang Z, Zhou XF, Zhang X, Zhu Q, Dong H, Zhao M, Oganov AR (2015) Nano Lett 15(9):6182
42. Pontes J, Frazão N, Azevedo DL, Lima JR (2021) Comput Mater Sci 188:110210
43. Shahrokhi M, Mortazavi B, Berdiyorov GR (2017) Solid State Commun 253:51
44. Ma XD, Tian ZW, Jia R, Bai FQ (2022) Appl Surf Sci 153674
45. Rublev P, Tkachenko NV, Boldyrev AI (2022) J Comb Chem
46. Karaush NN, Bondarchuk SV, Baryshnikov GV, Minaeva VA, Sun WH, Minaev BF (2016) RSC Adv 6(55):49505
47. Bianco A, Cheng HM, Enoki T, Gogotsi Y, Hurt RH, Koratkar N, Kyotani T, Monthioux M, Park CR, Tascon JM et al (2013) All in the graphene family–a recommended nomenclature for two-dimensional carbon materials
48. Clark SJ, Segall MD, Pickard CJ, Hasnip PJ, Probert MI, Refson K, Payne MC (2005) Zeitschrift für kristallographie-crystalline materials 220(5-6):567
49. Systèmes D (2017) San Diego
50. Perdew JP, Burke K, Ernzerhof M (1996) Phys Rev Lett 77:3865. https://doi.org/10.1103/PhysRevLett.77.3865. https://link.aps.org/doi/10.1103/PhysRevLett.77.3865
51. Heyd J, Scuseria GE, Ernzerhof M (2003) J Chem Phys 118(18):8207
52. Ljungberg MP, Vänskä O, Koval P, Koch SW, Kira M, Sánchez-Portal D (2017) New J Phys 19(3):033019. https://doi.org/10.1088/1367-2630/aa616d
53. Soler JM, Artacho E, Gale JD, García A, Junquera J, Ordejón P, Sánchez-Portal D (2002) J Phys: Condens Matter 14(11):2745
54. García A, Verstraete MJ, Pouillon Y, Junquera J (2018) Comput Phys Commun 227:51
55. Tromer RM, Felix LC, Ribeiro LA, Galvao DS (2021) Physica E 130:114683
56. Luo Y, Ren C, Xu Y, Yu J, Wang S, Sun M (2021) Sci Rep 11(1):1
57. Bafekry A, Faraji M, Fadlallah M, Jappor H, Karbasizadeh S, Ghergherehchi M, Gogova D (2021) J Phys: Condens Matter 34(1):015001
58. Pereira M, da Cunha W, de Sousa R, Nze GA, Galvão D, Ribeiro L (2022) Nanoscale 14(8):3200
59. Mortazavi B, Shapeev AV (2022) FlatChem 32:100347
60. Falin A, Cai Q, Santos EJ, Scullion D, Qian D, Zhang R, Yang Z, Huang S, Watanabe K, Taniguchi T et al (2017) Nat Commun 8(1):15815